Gear Lubrication and Cooling Experiment and Analysis*

Dennis P. Townsend† and Lee S. Akin‡

There are several methods of lubricating and cooling gear teeth: splash lubrication, drip feed, air/oil mist, and pressurized oil-jet flow. The method of successful lubrication usually depends on the operating conditions. For gears operating at moderate to high speed (above 5000 rpm), the pressurized oil jet becomes necessary to provide adequate lubrication and cooling and to prevent scoring of the gear-tooth surfaces. Scoring is a result of having a too thin elastohydrodynamic (EHD) oil film. This thin EHD film is usually caused by inadequate cooling rather than insufficient lubricant.

Of the three primary modes of gear tooth failure, scoring is the most common and the most difficult to analyze. A considerable amount of work has been done over the past four decades to produce quantitative analysis procedures to evaluate the risk of scoring in lubricated gear drives (refs. 1 and 2). For the first 30 years of this time period, most of the concentrated effort had to do with developing a procedure to evaluate the incipient onset of the scoring phenomenon. It has only been in the last decade or so that a concentrated effort has been provided to evaluate the contribution of the gear tooth bulk temperature on the scoring phenomenon and to determine its contribution in bringing about the onset of this mode failure of (refs. 3 and 4).

A computer program was developed using a finite-element analysis to predict gear tooth temperatures (refs. 5 and 6). However, that program did not include the effects of oil-jet cooling and oil-jet impingement depth. It used an average surface heat-transfer coefficient for surface temperature calculation based on the best information available at that time.

To have a better method for predicting gear-tooth temperature, it is necessary that the analysis allow for the use of a heat-transfer coefficient for oil-jet cooling coupled with a coefficient for air/oil mist cooling for that part of the time that each condition exists. Once the analysis can make use of these different coefficients, it can be combined with a method that determines the oil-jet impingement depth to give a more complete gear-temperature analysis program. However, both the oil-jet and air/oil mist heat-transfer coefficients are unknowns and must be determined experimentally.

The objectives of the work reported herein were to (1) further develop the gear-temperature analysis computer program (refs. 5 and 6), which incorporates different heat-transfer coefficients for air/oil and oil-jet cooling, (2) combine that program with a program developed to determine the impingement depths, and (3) experimentally measure gear-tooth temperatures to compare them with those predicted using the improved analysis.

Symbols

a	diffusivity, $= k/P\ C_p$, lb/in °F sec$^{1/2}$
b	Hertzian contact width, m (in.)
C_p	specific heat, J/kg K (Btu/lb °F)
d_i	oil-jet impingement depth, m (in.)
F_e	effective face width, m (in.)
f	friction coefficient
h_j	heat-transfer coefficient for lubricated flank of gear, W/hr m^2 K (Btu/hr ft^2 °F)

*Previously published in Journal of Mechanical Design, vol. 103, no. 4, Jan. 1981, pp. 219-226; also as NASA TM-81419 under the title "Analytical and Experimental Spur Gear Tooth Temperature as Affected by Operating Variables."

†NASA Lewis Research Center.

‡Western Gear Corp., Industry, Calif.; also California State University, Long Beach.

h_s heat-transfer coefficient sides of gear, W/hr m^2 K (Btu/hr ft^2 °F)
h_t heat-transfer coefficient for unlubricated flank of gear, W/hr m^2 K (Btu/hr ft^2 °F)
J heat conversion factor
k infrared radiometric microscope constant
L_A line of action length, m (in.)
L_t length of tooth, m (in.)
m module
N number of teeth
ΔN radiance
P_d diametral pitch module (in^{-1})
q heat flux, W/hr (Btu/hr)
q_t total heat generated, W/hr (Btu/hr)
V rolling velocity, m/sec (ft/sec)
ΔV infrared radiometric microscope measured, V
V_g gear pitch line velocity, m/sec (ft/sec)
V_j oil-jet velocity, m/sec (ft/sec)
V_s sliding velocity, m/sec (ft/sec)
W normal tooth load, N (lb)
W_t tangential tooth load, N (lb)
α oil-jet angle from radial, deg
β temperature coefficient of viscosity
δ_i dimensionless impingement depth, d_iP_d, m^2 (in.)
ϵ emissivity
η rotation angle, revolutions/sec
θ_s temperature, K (°F)
θ_w gear rotation angle from tip of tooth to impingement point, rad
κ thermal conductivity, W/m K (Btu/ft °F)
Λ partition constant
ν,ν_o kinematic viscosity
ν_j dimensionless oil-jet velocity
ρ density, kg/m^3 (lb/in^3)
$\rho_{1,2}$ involute radius of curvature, m (in.)
φ pressure angle, rad
ω angular velocity, rad/sec

Apparatus and Procedure

Gear Test Apparatus

Gear-tooth temperature measurements were made using the NASA gear test shown in figure 1 and described in reference 7. This test rig uses the four-square principle of applying the test gear load so that the input drive needs only to overcome the frictional losses in the system.

The gear surface temperatures were measured with a fast-response infrared radiometric (IR) microscope that uses a liquid-nitrogen-cooled detector. The IR microscope can measure transient temperatures up to 20 000 Hz. All radiance measurements were made with a 1 × lens that has a focal length of approximately 23 cm (9 in.) and a viewing spot size of 0.05 cm (0.020 in.) diameter. The test gear cover, viewing port, and lubrication jet as shown in figure 2 were used with the IR microscope.

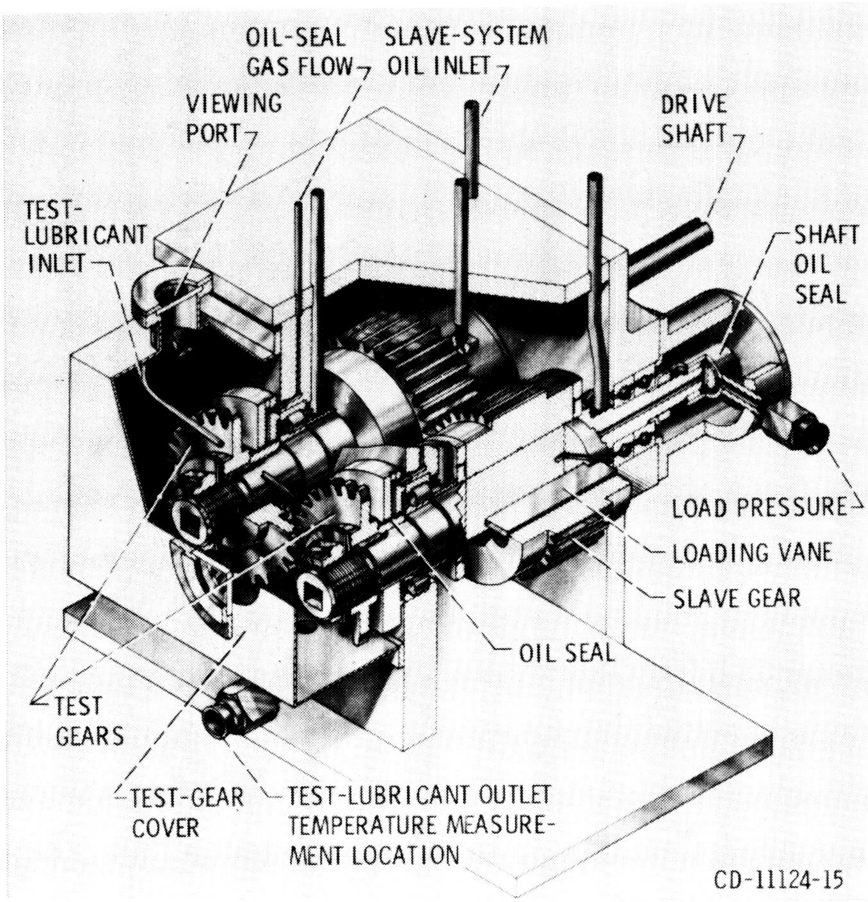

Figure 1. -NASA Lewis Research Center's gear fatigue test apparatus.

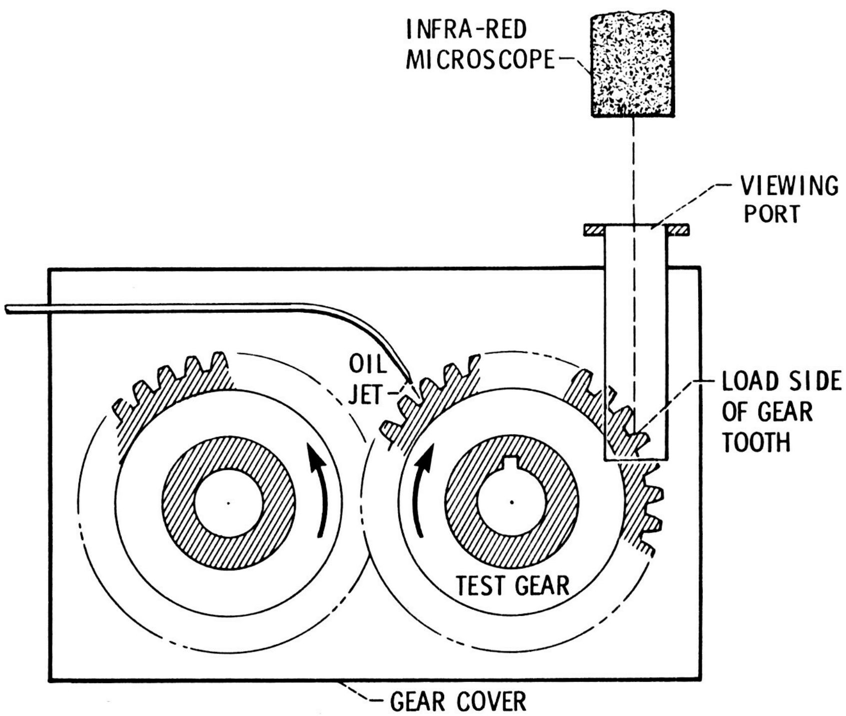

Figure 2. - Test setup for measuring dynamic gear tooth surface temperature.

Test Gears

The 28-tooth test gears were of 8 diametral pitch and 8.89-cm (3.5-in.) pitch diameter with a 0.635-cm (0.250-in.) face width. All gears had a nominal surface finish on the tooth flank of 0.406 μm (16 μin.), rms, and a standard 20 involute profile without tip relief. The test gears were manufactured from consumable-electrode vacuum-melted (CVM) AISI 9310 steel. The gears were case carburized and hardened to a Rockwell C hardness of 60 before final grinding of the finished gear.

Test Lubricant

The test gears were lubricated with a single batch of synthetic paraffinic oil. The physical properties of the oil are summarized in table I. Five percent of an extreme pressure additive, designated Lubrizol 5002, was added to the lubricant.

Test Procedure

After the test gears were cleaned to remove the preservative, they were assembled on the test rig. The test gears were run in a full face load condition on the 0.635-cm (0.250-in.) face width. The tests were run at four speeds, 2500, 5000, 7500, and 10 000 rpm; three tangential loads, 1895, 3736, and 5903 N/cm (1083, 2135, and 3373 lb/in.); five oil-jet pressures 96×10^4, 69×10^4, 41×10^4, 27×10^4, and 14×10^4 Pa (140, 100, 60, 40 and 20 psi); and two oil-jet diameters, 0.04 and 0.08 cm (0.016 and 0.032 in.). Inlet oil temperature was constant at 308 K (95° F). At each speed the lowest load was first applied with the maximum oil-jet pressure. At this load the oil-jet pressure was reduced in steps to the lowest pressure before the next load was applied. The oil jet was pointing in a radial direction and hitting the unloaded side of the gear tooth as it came out of the mesh zone. The 0.08-cm (0.032-in.) diameter jet is the size typically used in many applications for the maximum power conditions used herein. The 0.04-cm (0.016-in.) diameter jet was used to determine what cooling conditions could be obtained with considerably less oil flow and good oil-jet impingement depth. The temperature was measured by the IR scope at a location approximately 160° away from the mesh zone.

The IR scope operates in two modes. In the DC mode the average surface temperature of the gear tooth was read out on the meter supplied with the IR scope. The scope was calibrated before running the tests to determine the emissivity of the gear-tooth surface. In the AC mode a voltage that varies with surface radiance according to the equation

$$\Delta V = \kappa\epsilon\, \Delta N \tag{1}$$

was measured from two signals on a dual trace cathode-ray oscilloscope (CRO). The upper signal in figure 4 was from the IR scope directly; the lower signal was filtered through a variable-band-pass filter to remove the 20-mV high-frequency noise. At the lower loads and at the high oil-jet pressure, the signal-to-noise ratio was approximately one.

The gear-tooth surface was viewed by the IR scope as it passed before the lens. The tip of the tooth is seen first; the view then goes down the tooth surface until it is interrupted by the next tooth.

TABLE I - LUBRICANT PROPERTIES OF SYNTHETIC PARAFFINIC OIL PLUS ADDITIVES[a]

Kinematic viscosity, cm^2/sec (cs) at:	
244 K (-20° F)	2500×10^{-2} (2500)
311 K (100° F)	31.6×10^{-2} (31.6)
372 K (210° F)	5.7×10^{-2} (5.7)
477 K (400° F)	2.0×10^{-2} (2.0)
Flash point, K (°F)	508 (455)
Fire point, K (°F)	533 (500)
Pour point, K (°F)	219 (-65)
Specific gravity	0.8285
Vapor pressure at 311 K (100° F), mm Hg (or torr)	0.1
Specific heat at 311 K (100° F), J/(kg)(K)(Btu/(lb)(°F)	676 (0.523)

[a]Additive, Lubrizol 5002 (5 vol. %). Additive content: phosphorus, 0.6 wt %; sulfur, 18.5 wt %.

Gear Temperature Analysis

A gear-tooth temperature analysis was developed in references 5 and 6 to calculate the gear-tooth temperature profile using a finite-element analysis. This analysis uses a finite-element mesh and calculates isotherms on the gear tooth. However, the following conditions are required to be determined or calculated before the program can calculate effective temperatures: (1) the frictional heat input at the gear-tooth working surface, (2) the different heat-transfer coefficients for the various gear-tooth surfaces and cooling methods, and (3) the oil-jet penetration onto the gear-tooth flank.

The frictional heat input to the gear-tooth working surface can be calculated using the following analysis: The instantaneous heat generated per unit area per unit time due to the sliding of the two gear teeth is given by

$$q=\frac{fW\left|V_s\right|}{bJ}=\frac{fW\left|\omega_1\rho_1-\omega_2\rho_2\right|}{bJ} \tag{2}$$

where

$$W=\frac{W_t}{F_e}\cos\varphi$$

Since W, V_s, *and* f are functions of the mesh-point location, the q will vary through the meshing cycle. The f varied from approximately 0.02 to 0.07 for the cases evaluated. The heat generated will be divided between the gear and pinion and may not be equally withdrawn by each, so that a partitioning function Λ is used. The heat withdrawn by the gear and pinion will then be

$$q_1=\Lambda q \qquad q_2=(1-\Lambda)q \tag{3}$$

For the test gears used in this paper Λ is assumed to be 0.5, so that

$$q_1=q_2 \tag{4}$$

once the instantaneous heat flux to the gear surface is determined. The total time average heat flow per revolution can be calculated by the following equation from reference 6:

$$q_1=\frac{b\omega_1\Lambda}{V_1 2\pi}=\frac{b\omega_2(1-\Lambda)q}{V_2 2\pi} \tag{5}$$

where V_1 and V_2 are the gear and pinion rolling velocities. Substituting equation (2) into equation (5) gives

$$q_1=q_2=\frac{\Lambda fW_1^2}{V_1 2\pi J}\rho_1-\frac{\omega_2}{\omega_1}\rho_2 \tag{6}$$

substituting

$$\Lambda=0.5,\ \eta_1=\frac{\omega_1}{2\pi},\ \frac{\omega_2}{\omega_1}=\frac{N_1}{N_2},\ \text{and } V_1=\omega_1\rho_1$$

gives

$$q_1=q_2=\frac{fW\eta_1}{2J}\left|1-\frac{N_1}{N_2}\frac{\rho_2}{\rho_1}\right| \tag{7}$$

for the time-averaged heat flux. Using this expression, the instantaneous heat flux may be calculated at any position along the line of action by substituting the instantaneous profile radius, giving the heat input to the gear-tooth surface at that location. Substituting $L_A - \rho_1$ for ρ_2, where $L_A = \rho_1 + \rho_2$, and using instantaneous notation, equation (8) becomes

$$q_{i1} = \frac{f_i W \eta_1}{2J} \left| 1 - \frac{N_1}{N_2} \left(\frac{L_A - \rho_{i1}}{\rho_{i1}} \right) \right| \tag{8}$$

The heat-transfer coefficients (fig. 3) for the sides, top land, and flanks of the gear teeth are different because of the different cooling regions. Also, the coefficient for the two flanks will be different, depending on whether they are cooled by the oil-jet hitting the surface or by air (no jet cooling). The heat-transfer coefficient for the sides of the gear teeth h can be estimated by the method of reference 9 for a rotating disk by

$$h_s = \mathrm{Nu}\ \kappa \sqrt{\frac{\omega}{V}} \tag{9}$$

where for air Nu = 0.5. However, the amount of oil mist present will have a considerable effect on this coefficient. The gear-tooth flanks not cooled by the oil jet will have a heat-transfer coefficient h_t for air or air/oil mist. Since there are no data available to determine this coefficient, an estimate somewhere between air cooling and jet cooling will be used until something better is obtained experimentally.

The heat-transfer coefficient h_j for the jet-cooled tooth face and the tooth tip may be calculated (refs. 4 and 8) using the following equation:

$$h_j = \left(\frac{2L_t}{m} \right)^{1/4} \left(\frac{\nu_o}{aN} \right)^{1/4} \frac{b\omega^{1/2}}{2\pi} q_{\mathrm{tot}} \tag{10}$$

where q_{tot} is a dimensionless factor (refs. 4 and 8). Curve fitting the data (ref. 8) gives

$$q_{\mathrm{tot}} = 0.98 = 0.32\,\gamma + 0.06\,\gamma^2 - 0.004\,\gamma^3 \tag{11}$$

where

$$\gamma = \beta \theta_s \tag{12}$$

Using the above method for calculating the oil-jet heat-transfer coefficient gives temperatures that are much too high. For the results presented in this paper, an oil-jet heat-transfer coefficient was assumed that would give more realistic results. For future work a more realistic oil-jet heat-transfer coefficient will be determined based on experimental results reported in this paper and from future testing.

The oil-jet penetration onto the gear-tooth flank can be determined by the method of references 10 and 11. A more accurate analysis is being developed by the authors using a new kinematic radial model instead of the vectorial model used in reference 10. The new model gives the oil-jet impingement depth for radially directed jet as

$$\delta_i = \frac{v_j \theta_\omega (N+2) \cos \alpha}{4} \tag{13}$$

Using the above equation with a known jet velocity, the angle of rotation is assumed and must be iterated until the angle of rotation and inpingement point coincide, since θ_ω is a function of δ_i and θ_ω:

$$V_j = \frac{4\delta_i}{\theta_\omega (N+2) \cos \alpha} \tag{14}$$

Once the heat generation and the oil-jet impingement depth have been calculated, the heat-transfer coefficients are either calculated or estimated. Then, the finite-element analysis is used to calculate the temperature profile of the gear teeth. The finite-element model has 108 nodes with triangle elements. The computer program calculates a steady-state temperature at all 108 nodes and prints these temperatures. The program also plots temperature isobars on the gear-tooth profile and lists the temperatures of the isobars.

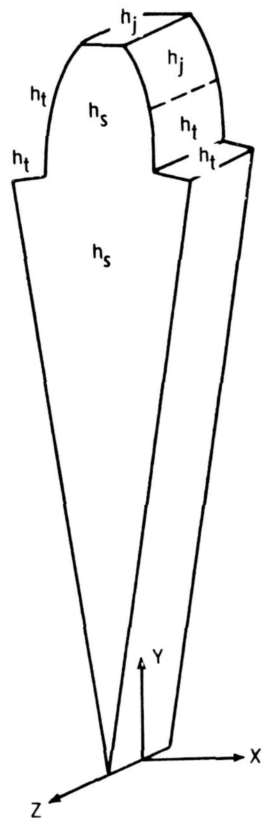

Figure 3. - Geometry of problem.

Results and Discussion

Experimental Results

Transient and average gear-tooth surface temperatures were measured using a fast-response infrared (IR) radiometric microscope. The gear-tooth temperatures were measured at four speeds, three loads, five oil-jet pressures, and two oil-jet diameters. The test gears were of 3.2 module (8 pitch), 8.89-cm (3.5-in.) pitch diameter with a 0.64-cm (0.25-in.) face width.

Figure 4(a) is a typical transient measurement of a gear tooth surface at 7500 rpm, 5903-N/cm (3373-lb/in) tangential load, and 14×10^4-Pa (20-psi) oil-jet pressure with a 0.041-cm (0.016-in.) diameter orifice. The change in surface temperature from the gear tooth tip to a point just below the pitch line was 32 K (58° F). The pitch line where pure rolling occurs can be seen by the slight dip in temperature. The highest temperature is below the pitch line where the combination of high load with some sliding occurs.

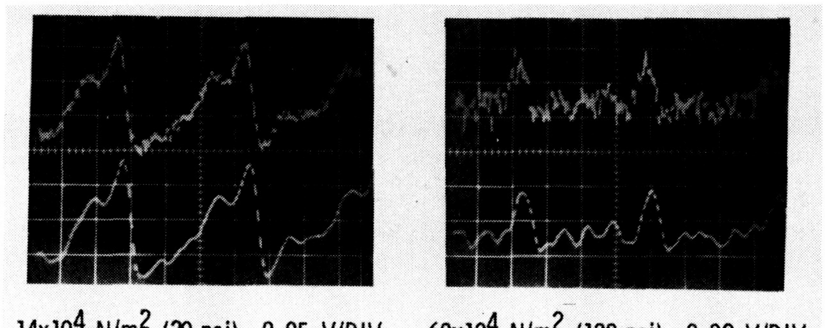

Figure 4. - IR microscope measurements of gear tooth surface temperature. Speed, 7500 rpm; load, 5903 N/cm (3373 lb/in); inlet oil temperature, 308 K (95° F); oil-jet diameter, 0.04 cm (0.016 in.).

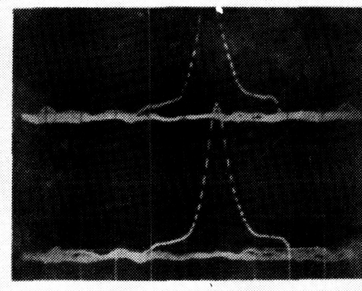

Figure 5. - IR microscope measurements of gear teeth scoring temperature. 0.5 V per division; speed, 10 000 rpm; load, 5903 N/cm (3373 lb/in); inlet oil temperature, 308 K (95° F); oil jet diameter, 0.04 cm (0.016 in.).

Figure 4(b) is for the same load, speed, and oil-jet size condition but with an oil-jet pressure of 97×10^4 Pa (140 psi), which reduces the maximum temperature difference to 12 K (22° F), with the peak temperature still occurring below the pitch line. The average surface temperature for these conditions was 423 and 391 K (302° and 244° F) for the 14×10^4- and 97×10^4-Pa (20- and 140-psi) oil pressures, respectively. Figure 5 is typical of what happens when scoring occurs. Here, the peak temperature is at the tip of the gear tooth and has reached a maximum temperature of 508 K (455° F) or 75 K (135° F) above the average surface temperature of 433 K (320° F). Scoring temperatures as high as 603 K (626° F) were measured during the high-load, high-speed tests with reduced oil-jet pressure or orifice size. These temperatures would be somewhat lower than those at the contact point, since they were measured 160° away from the contact and after oil-jet cooling. The scoring conditions occurred only at the 10 000-rpm test condition with intermediate loads and full or less oil-jet impingement depths.

Figure 6(a) is a plot of gear-tooth average surface temperature (solid line) with the high and low temperatures included (dashed lines) versus oil-jet pressure for three speeds, an oil-jet diameter of 0.04 cm (0.016 in.), and a load of 5903 N/cm (3373 lb/in).

The high load and high speed with the small jet size could not be run except at the highest pressure because of scoring. From these plots the effect of different speeds at constant load and the effect of oil-jet pressure on both average surface temperature and temperature variations can be seen. The increased speed causes a higher surface temperature and higher temperature variations. The oil-jet pressure also has a greater effect at the higher speed. The maximum oil pressure needed for a speed is also seen by the leveling of the curve at the lower speeds where increased oil pressure causes very little improvement in cooling.

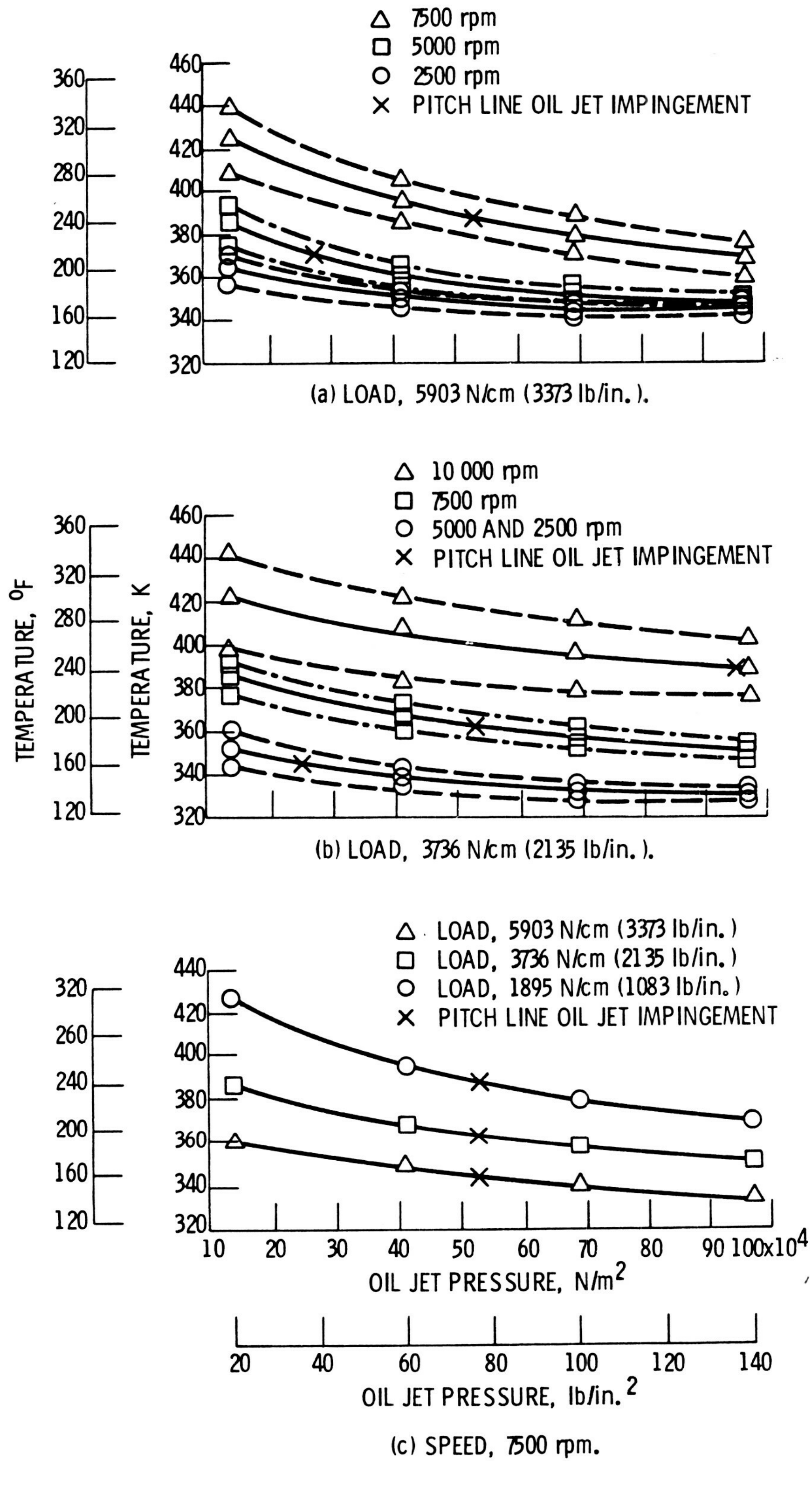

Figure 6. - IR microscope measurements of gear teeth surface temperature versus oil-jet pressure. Inlet oil temperature, 308 K (95° F); oil jet diameter, 0.04 cm (0.016 in.).

Figure 6(b) is the same type of plot as figure 6(a) except the load is 3736 N/cm (2135 lb/in). The curves for 5000 and 2500 rpm are nearly identical. The effect of oil-jet pressure is considerably reduced because of the lower load. Here, the maximum change in average surface temperature is 35 K, and the maximum surface temperature difference is 45 K at the 13.8×10^4-Pa (20-psi) oil-jet pressure.

Figure 6(c) is a plot of gear-tooth average surface temperature versus oil-jet pressure with different loads at a speed of 7500 rpm. This figure shows the effect of load and oil-jet pressure on gear-tooth temperature at constant speed.

Figure 7 is a plot of load versus gear-tooth average surface temperature for the 7500 rpm condition and three oil-jet pressures. The effect of load and oil-jet pressure on gear-tooth surface temperature is clearly seen. Increasing the pressure from 14×10^4 to 97×10^4 Pa (20 to 140 psi) has about the same effect as reducing the load from 6000 to 2000 N/cm.

Figure 8 shows plots of average surface temperatures with temperature variations and bulk gear temperature, respectively, versus oil-jet pressure for three loads at 10 000 rpm and an oil-jet size of 0.08 cm (0.032 in). With the larger oil-jet size, the temperatures are reduced considerably from those with the smaller jet size. The bulk temperature of the gear does not increase as much as the average surface temperature. At the lower load and high jet pressure, the surface and bulk temperatures are nearly identical.

Analytical Results

Calculations were made using the computer program to examine the effects of calculated heat inputs from the experimental test cases and estimated heat-transfer coefficients. The differential temperature profiles are shown in figures 9 to 11. The differential profiles in these figures are the temperature difference between the inlet cooling oil and the actual gear-tooth temperatures.

Matching the analytical predictions with the experimental results is difficult because of different physical conditions existing in the program input and the experiment. The analysis and the tests were planned whereby heat removal was on the working face of the gear tooth. The analysis was completed before the tests were conducted. Initial testing resulted in oil splashing on the infrared microscope viewing port, which prevented meaningful IR temperature measurements. To prevent this condition from occurring, the oil jet was directed at the back side of the tooth, resulting in cooling of the unloaded side of the gear tooth.

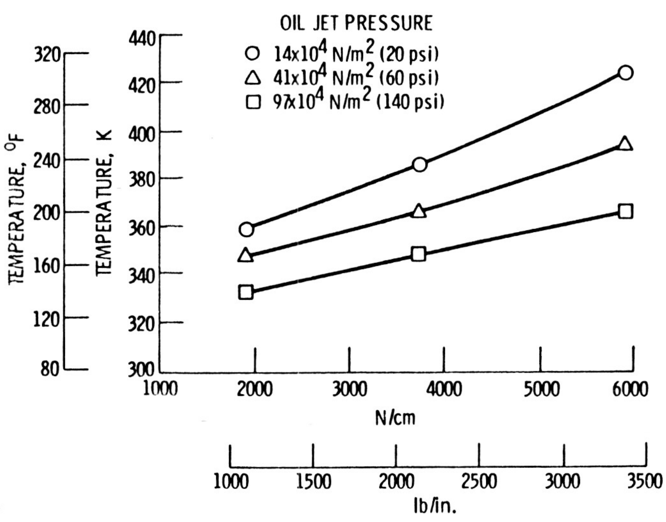

Figure 7. - IR microscope measurements of gear average surface temperature versus load for three oil-jet pressures. Speed, 7500 rpm; oil-jet diameter, 0.04 cm (0.016 in.); inlet oil temperature, 308 K (95° F).

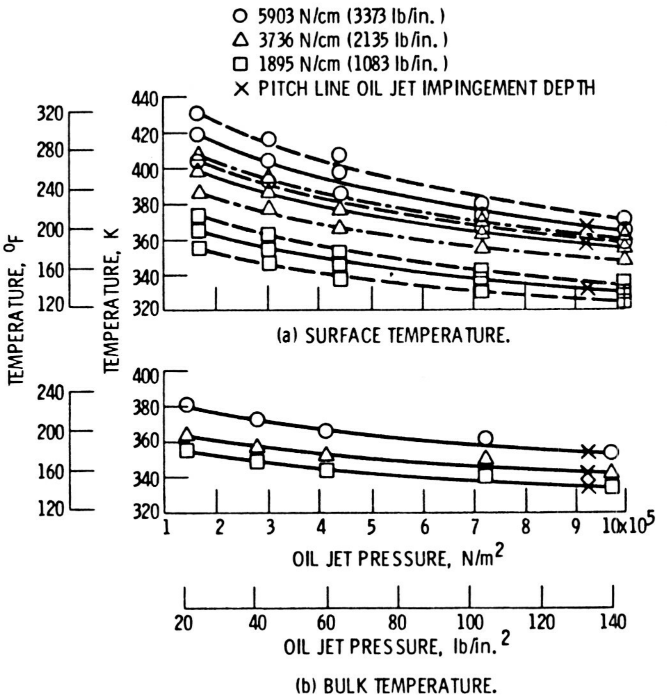

Figure 8. - IR microscope and thermocouple measurements of gear temperature versus oil-jet pressure for three loads. Speed, 10 000 rpm; oil-jet diameter, 0.08 cm (0.032 in.); inlet oil temperature, 308 K (95° F).

The conditions of figure 9(a) were 10 000 rpm with a tangential tooth load of 5903 N/cm (3373 lb/in) and an impingement depth of zero. This means that the gear had impingement on the top land only. The lowest level of temperature difference in the gear tooth is 35 K (63° F) at the tip of the tooth. The hot spot is just below the pitch line and is 122 K (200° F) above the oil-jet temperature. This gives an average surface temperature above oil-jet temperature of approximately 79 K (142° F).

Figure 9(b) is a gear-tooth temperature profile for the same conditions as figure 9(a) except that the oil-jet impingement is 87.5 percent of the tooth depth. Here, the minimum temperature difference is at the tooth tip of 9 K (16° F), and the highest temperature difference just below the pitch line is 31 K (56° F).

Figure 10(a) is the analytical results for an operating condition of 7500 rpm, a tangential tooth load of 1895 N/cm (1083 lb/in) and an impingement depth of zero. The minimum temperature difference between the oil-jet and tooth temperature is at the tooth tip and is 16 K (29° F), while the maximum temperature of 50 K (90° F) is below the pitch point.

Figure 10(b) is the same conditions as figure 10(a) except for the oil-jet impingement depth of 87.5 percent of the tooth depth. The minimum and maximum oil-jet to gear-tooth temperatures are 4 and 12 K (7° and 22° F).

Figure 11 shows the analytical results for cooling on the back (or unloaded) side of the gear tooth in a manner to match that obtained in the experiment. The minimum and maximum calculated oil-jet gear-tooth temperatures of 92 and 127 K (166° and 229° F) at 33.5 percent depth are fairly close to the experimentally measured temperatures of 95 and 123 K (171° and 221° F), respectively. Likewise for the 75.3 percent depth, where the minimum and maximum calculated temperatures of 43 and 70 K (77° and 126° F) were close to the experimentally measured temperatures of 49 and 63 K (88° and 113° F), respectively.

With the analytical results using backside cooling and the experimentally adjusted film coefficients, the calculated and experimental temperatures are in very good agreement. The analytical results of figures 9 and 10, obtained for cooling on the loaded side of the tooth, show only fair agreement with the experimental results, which were for cooling on the backside of the teeth, resulting in inaccurate estimates of the heat-transfer coefficients.

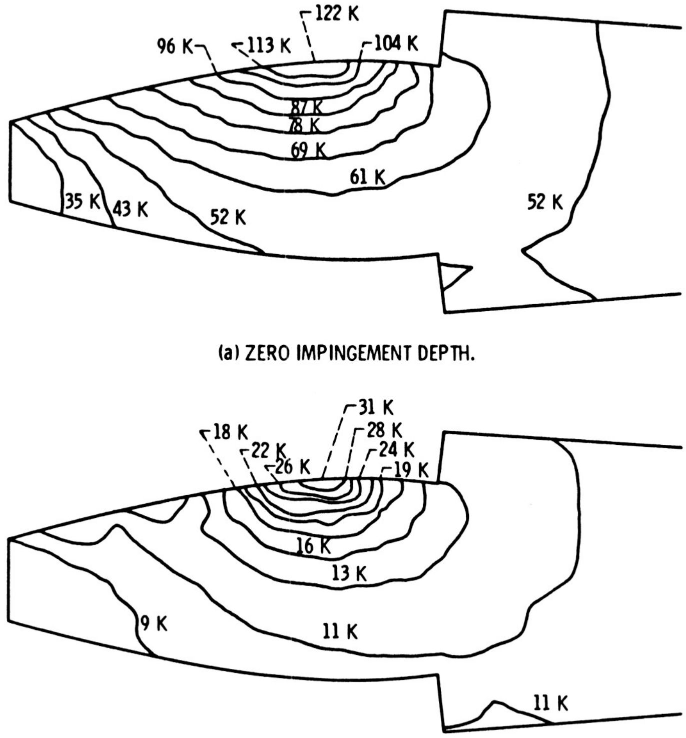

(a) ZERO IMPINGEMENT DEPTH.

(b) 87.5 percent IMPINGEMENT DEPTH.

Figure 9. - Calculated gear tooth temperatures. Speed, 10 000 rpm; load, 5903 N/cm (3373 lb/in).

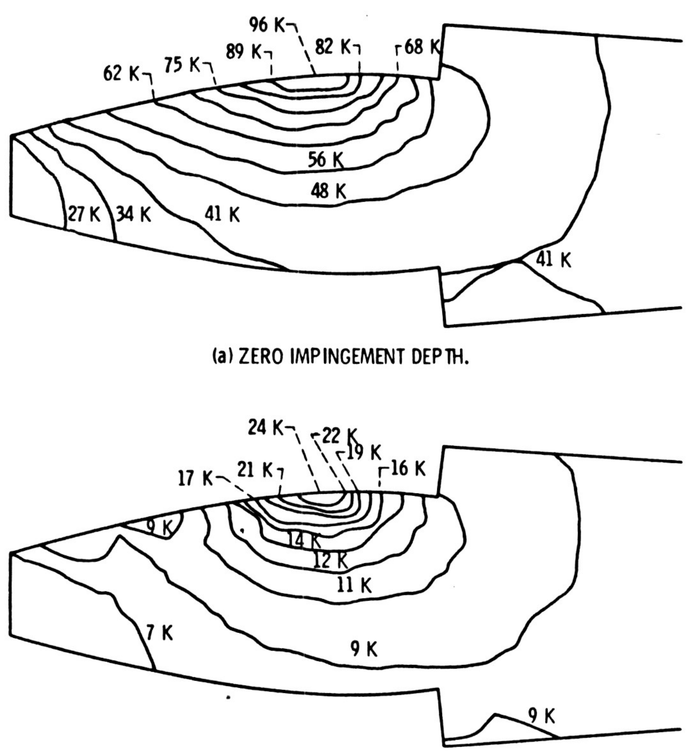

(a) ZERO IMPINGEMENT DEPTH.

(b) 87.5 percent IMPINGEMENT DEPTH.

Figure 10. - Calculated gear tooth temperatures. Speed, 7500 rpm; load, 1875 N/cm (1083 lb/in)

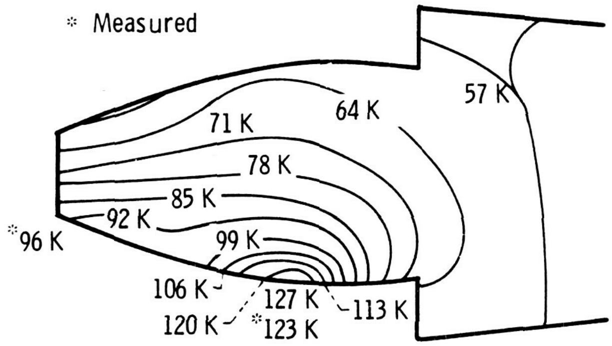

(a) 33.5 percent impingement depth.

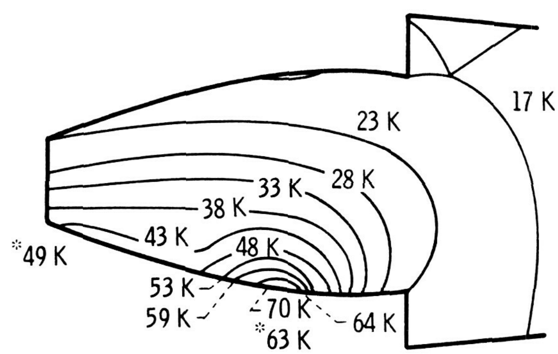

(b) 75 percent impingement depth.

Figure 11. - Calculated gear tooth temperatures for gears cooled on backside. Speed, 10 000 rpm; load, 5903 N/cm (3373 lb/in).

Summary of Results

A gear-tooth temperature analysis was performed using a finite-element method combined with a calculated heat input, a calculated oil-jet impingement depth, and estimated heat-transfer coefficients for the different parts of the gear tooth that are oil cooled and air cooled. Experimental measurements of gear-tooth average surface temperature and gear-tooth instantaneous surface temperature were made with a fast-response, infrared, radiometric microscope. The following results were obtained.

1. Increasing oil pressure has a significant effect on both average surface temperature and peak surface temperature at loads above 1895 N/cm (1083 lb/in) and speeds of 10 000 and 7500 rpm.
2. Both increasing speed (from 5000 to 10 000 rpm) at constant load and increasing load at constant speed cause a significant rise in the average surface temperature and in the instantaneous peak surface temperatures on the gear teeth.
3. The oil-jet pressure required to provide the best cooling for gears is the pressure required to obtain full gear-tooth impingement.
4. Calculated results for gear tooth temperatures were close to experimental results for various oil-jet impingement depths for identical operating conditions.

References

1. Blok, H.: Lubrication as a Gear Design Factor. Proc. International Conference on Gearing. The Institution of Mechanical Engineers, 1958.
2. Kelley, B. W.; and Lemanski, A. J.: Lubrication of Involute Gearing. Proc. Inst. Mech. Eng. (London), vol. 182, pt. 3A, 1967-1968, pp. 173-184.
3. Akin, L. S.: An Interdisciplinary Lubrication Theory for Gears (With Particular Emphasis on the Scuffing Model of Failure). J. Eng. Ind., vol. 95, no. 4, Nov. 1973, pp. 1178-1195.
4. DeWinter, A.; and Blok, H.: Fling-Off Cooling of Gear Teeth. J. Eng. Ind., vol. 96, no. 1, Feb. 1974, pp. 60-70.
5. Wang, K. L.; and Cheng, H. S.: A Numerical Solution to the Dynamic Load, Film Thickness, and Surface Temperatures in Spur Gears, Part II—Results. Presented at the ASME International Power Transmission and Gear Conference, Chicago, Sep. 28-30, 1977.
6. Patir, N.; and Cheng, H. S.: Prediction of Bulk Temperature in Spur Gears Based on Finite Element Temperature Analysis. ASLE Preprint No. 77-LC-3B-2, Oct. 1977.
7. Townsend, D. P.; Bamberger, E. N.; and Zaretsky, E. V.: A Life Study of Ausforged, Standard Forged, and Standard Machined AISI M-50 Spur Gears. J. Lubr. Technol., vol. 98, no. 3, July 1976, pp. 418-415.
8. Van Heijningen, G. J. J.; and Blok, H.: Continuous as Against Intermittent Fling-Off Cooling of Gear Teeth. J. Lubr. Technol., vol. 96, no. 4, Oct. 1974, pp. 529-538.
9. Patir, N.: Estimate of the Bulk Temperature in Spur Gears Based on Finite Element Temperature Analysis. M.S. Thesis, Northwestern University, 1976.
10. Akin, L. S.; Mross, J. J.; and Townsend, D. P.: Study of Lubricant Jet Flow Phenomena in Spur Gears. J. Lubr. Technol., vol. 97, no. 2, Apr. 1975, pp. 283-288.
11. Townsend, D. P.; and Akin, L. S.: Study of Lubricant Jet Flow Phenomena in Spur Gears—Out of Mesh Condition. J. Mech. Des., vol. 100, no. 1, Jan. 1978, pp. 61-68.